

Application of Makyoh (magic-mirror) topography in the research of artificial biomineralization

F. RIESZ^{a*}, L. PRAMATAROVA^b, E. V. PECHEVA^b, M. DIMITROVA^b

^a*Hungarian Academy of Sciences, Research Institute for Technical Physics and Materials Science, P. O. Box 49, H-1525 Budapest, Hungary*

^b*Institute of Solid State Physics, Bulgarian Academy of Sciences, 72 Tzarigradsko Chaussee Blvd., 1784 Sofia, Bulgaria*

The use of Makyoh (magic-mirror) topography (MT), an optical surface characterisation tool, is demonstrated in the research of artificial biomineralisation. The method is based on the defocused detection of the whole-sample reflection of collimated light. The sample surface morphology is revealed in the form of dark/bright contrast regions in the reflected image, due to the focusing/defocusing action of the morphological features of the surface. It is shown that MT can be used for the quick, qualitative assessment of the mm and sub-mm scale morphology of the substrates used for deposition of hydroxyapatite layers. In particular, we show the roughening effect in stainless steel substrates due to Ca+P implantation.

(Received November 28, 2006; accepted December 21, 2006)

Keywords: Biomineralisation, Hydroxyapatite, Surface morphology, Makyoh topography

1. Introduction

The deposition of hydroxyapatite (HA) layers is a common way to tailor surfaces to be bioactive and biocompatible, for applications as human implants or sensors [1]. The abundance of the used substrate materials, surface preparation technologies and deposition methods requires different methods for the multi-faceted characterisation of the physical, chemical, morphological and mechanical properties of the used substrates and deposited layers.

In particular, surface morphology is of crucial importance for a proper nucleation and attachment of the HA layers [2]. Various methods, such as optical and scanning electron microscopy and scanning probe methods, are used for the study of the morphology. In this paper, the use of Makyoh (magic-mirror) topography (MT), an innovative, powerful optical surface characterisation tool, is demonstrated in the morphological studies of artificial biomineralisation.

2. Background and general considerations

MT, which is based on the principle of the ancient mirror of Far-Eastern origin, is a powerful topographic tool for the qualitative visualization of the surface morphology of specular surfaces [3]. Its operation is the following: the sample is illuminated by a uniform collimated light beam, and the reflected beam is intersected by a screen on which an image of the sample is formed. The irregularities of the sample surface act as convex/concave mirror regions and focus/defocus the reflected beam, and the sample surface morphology is revealed in the form of bright/dark contrast regions in the image. The key parameter of imaging is the screen-to-sample distance, L . MT is applied mainly for the

qualitative inspection of the surface quality of semiconductor wafers [4].

MT can be made quantitative by applying structured illumination (e.g. by inserting a square grid into the path of the illuminating beam) [5]. The shift of the position of the grid's image as compared to the flat-sample case is proportional to the local gradient of the surface, from which the surface shape can be calculated by integration. This method can only be applied to study large-scale surface shapes.

The above simple picture is valid for specular surfaces, whose reflectivity and surface topography changes slowly (typically, semiconductor wafers). A general surface may be described as a combination of the following ones:

Specular surfaces with slowly varying reflectivity and surface topography: the case discussed above; the classic application of MT.

Microscopically rough, but reflecting surfaces. The interference of the beams reflected from the surface irregularities produces a random spotty pattern on a distant screen, known as speckle [6]. The average speckle size is given by $\lambda L/D$ where D is the size of the sample (or surface area from where reflection comes) and λ is the wavelength of the illumination.

Structured surfaces with macroscopically varying reflectivity. Abrupt reflectivity transitions cause diffraction fringes in the image. Modelling the reflectivity transitions as Fresnel diffraction at a half plane [4], the intensity maximum of the first fringe is situated at $w = 0.875(\lambda L)^{1/2}$. The extension of the well visible fringes is roughly $5w$. In samples with regions of steeply varying reflectivity, diffraction features can dominate a part of or even the whole image.

Surfaces that absorb or highly diffusely reflect light: no or a very faint reflected image.

Thus, each of the above surface features produces a characteristic image region, which, with some aid, provided by the sample's history, can be usually

distinguished from each other. (In principle, a given sample with macroscopically uniform properties – surface treatments, layer thickness etc. – should exhibit a uniform morphology on the large scale; however, non-ideal experimental conditions may lead to non-uniformities and the task of the measurement is just to assess these. On the other hand, combinatorial approaches, where the sample's different areas are deliberately exposed to different treatments, naturally lead to great morphological differences within a single sample.) A useful measurement practice is to continuously vary L while observing the MT image. At $L = 0$ we have the reflectivity map, which usually brings also some information about the surface (contamination, defects etc.). Increasing L increases the Makyoh contrast, due to surface topography; also, interference fringes appear, and the speckle size increases. An optimum L thus can be found and the contrast components due to reflectivity variations and the surface topography can be separated.

Diffraction features limit the maximum sample size as well, because of the fringe system produced at the sample edges. Approximating the sample edges again as half planes, stipulating that the fringes ($5w$, see above) should not cover more than 20% of the sample area at each edge, the minimum sample size d at a given L for a 820 nm wavelength is $d \approx [L] (1.3 \text{ mm})^{1/2}$.

Note also that in MT, white-light or partially coherent illumination is often used. Partial coherency decreases the visibility (contrasts) of the speckle and diffraction fringes.

3. Experimental

3.1. Makyoh topography system

Our experimental system is described in [4], in detail. We use a 820-nm pigtailed LED for illumination, a converging lens placed above the sample for collimation and as a „magnifier”, and a 800×600 pixel CCD camera connected to a PC, for visualisation. L can be set between 500 mm and 750 mm, by changing the distance setting of the camera lens. The maximum sample diameter is 20 mm in the settings we used, and the spatial resolution (distance per pixel) is about $50 \mu\text{m}$. A projected grid was used for large scale surface shape measurements.

3.2. Samples

During the course of our research, we have investigated over 150 samples, which can be classified as follows:

1. Bare substrates of polished silica glass (SG), stainless steel (SS) and n -type (100) Si wafers, as well as natural opal. The samples were polished as described in [7] (p. 18) and [8] for opal.

2. Substrates of SS, SG and Si, as described above, modified by Ca and P sequential ion implantation with energies and doses discussed in [7] (p. 25), and by thermal treatment following the ion implantation.

3. Samples with HA layers grown by soaking the substrates (bare and modified) in simulated body fluid (SBF) under biological conditions (ion composition of the fluid, ion concentrations, pH and temperature as those of the human blood plasma, see [7], p. 20). The soaking times ranged from four hours to six days.

4. Results and discussion

4.1. Bare substrates

SG samples are transparent at the wavelength we used. However, some reflection was visible at increased illuminating powers. We found the samples to be flat and essentially featureless. Figure 1 shows typical MT images at $L = 0$ and $L = -160$ mm. The only remarkable features are the diffraction features caused by surface defects and contamination. All other materials gave strong reflections. Si substrates also showed flat surfaces with very faint surface undulations on the sub-mm scale, typical of polished semiconductor wafers [4] (Fig. 2). Note that a weak periodic spotty pattern is present at $L = 0$, which can be attributed to cleaning residuals; the spotty pattern of the nonzero L image could partly be due to this reflectivity variation.

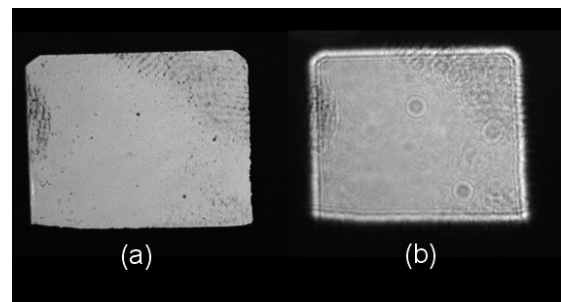


Fig. 1. Makyoh images of a 8×10 mm silica glass substrate at: (a) $L = 0$; (b) $L = -160$ mm.

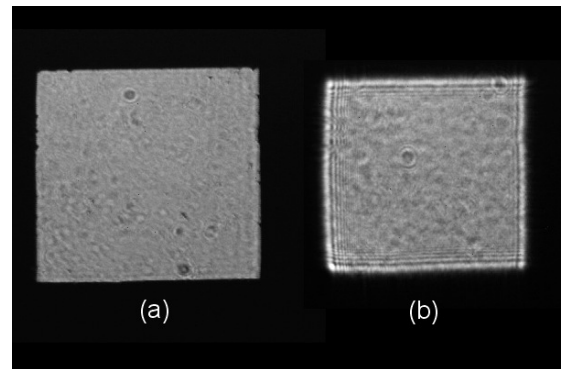


Fig. 2. Makyoh images of a 10×10 mm silicon substrate at: (a) $L = 0$; (b) $L = -160$ mm.

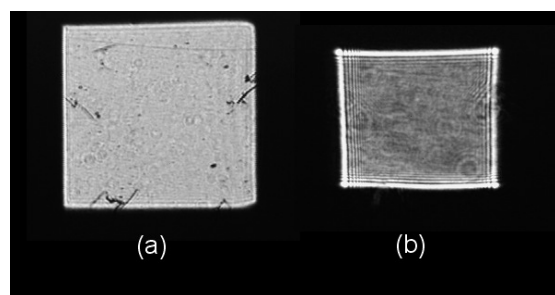


Fig. 3. Makyoh images of a 10×10 mm stainless steel substrate at: (a) $L = 0$; (b) $L = -160$ mm.

SS substrates also showed some roughness on the mm scale (Fig. 3). In addition, various surface defects (pits, scratches) could be identified on the $L = 0$ image.

The MT image of natural opal at $L = 0$ (Fig. 4a) revealed the presence of two zones: a thin transparent band (visible on the right hand side of the sample) and a central white-coloured part. These regions were identified as microcrystalline quartz, with inclusions of morganite in the transparent band, and mixed layering of crystalline cristobalite, crystalline quartz and tridymite in the white region [8]. The image for $L = 0$ shows a fine structure, hinting at roughness created by polishing. The image at $L = -160$ mm (Fig. 4b) shows a more pronounced spotty pattern due to the surface roughness. In addition, curved lines appear, probably related to some structural surface features or mechanical stresses (note that these lines are not visible on the $L = 0$ image).

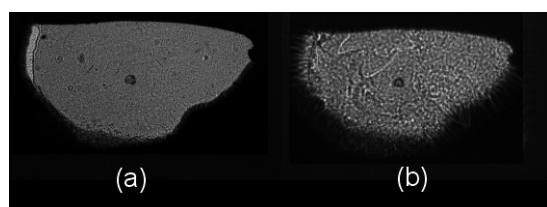


Fig. 4. Makyoh images of a 15×10 mm natural opal substrate at: (a) $L = 0$; (b) $L = -160$ mm.

We have also studied the large-scale surface shape using the projected grid. The opal, SG and Si substrates were flat (curvature radius usually greater than 30 m). SS samples exhibited various shapes (e.g., sphere, cylindrical, saddle) with characteristic curvature radii in the range of approximately 2 m to infinity, with no obvious correlation with the parameters of surface modification technologies.

4.2. Surfaces modified by ion implantation

It was observed for SS substrates that implantation caused macroscopically observable roughening of the surface on the sub-mm scale. Annealing at 600°C for 1 h in air caused partial smoothing (Fig. 5; the large spots in the images are traces of sputtering from depth elemental analysis). No changes as a result of implantation were observed in Si and SG substrates, within the limits of the MT method. Note that this result complements our

previous AFM studies: ion implantation induced a much higher microscopic roughness on the SS substrates (from 45 to 350 nm), evaluated in a $5 \mu\text{m} \times 5 \mu\text{m}$ area) in comparison to the Si and SG surfaces (from 5 to 15 nm, evaluated in a $1 \mu\text{m} \times 1 \mu\text{m}$ area) (p. 34 in [7]). Roughening thus occurs not only on the microscopic but also on a much larger macroscopic (sub-mm) length scale.

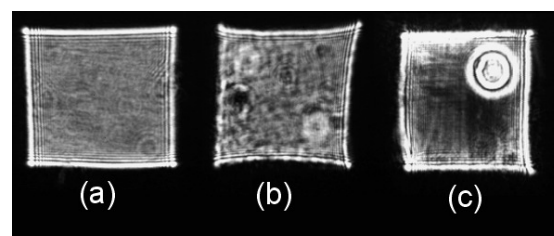


Fig. 5. Makyoh images of SS substrates at $L = -160$ mm: (a) virgin; (b) implanted with Ca+P ions; (c) annealed.

4.3. Samples with overgrown HA layers

HA layers grown on SG with 18 hour soaking times in SBF appeared matt to the naked eye. These layers gave a low (practically undetectable) reflection in MT. On the other hand, opal substrates with HA layers grown with a 18-hour soaking time were reflective and gave well defined images. Inhomogeneities of the HA thickness are revealed as differences in the reflectivity (Fig. 6). For example, bubble formation during the HA deposition process was observed as dark round spots in the MT images. The small white dots are small crystallites of HA whose reflectivity is greater, as confirmed by optical microscopy. Increasing L yields only a defocus of the image and no additional information, confirming that the image contrast results solely from reflectivity differences.

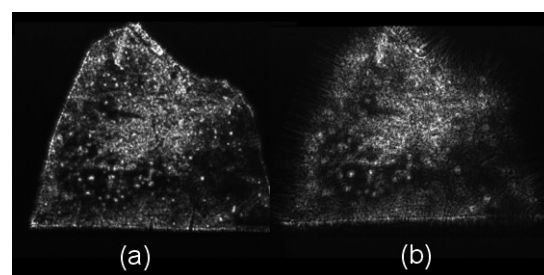


Fig. 6. Makyoh images of a HA layer grown on the opal substrate at: (a) $L = 0$; (b) $L = -160$ mm.

5. Conclusions

MT can be used for the quick, qualitative assessment of the gross mm-scale morphological and reflection features of substrates used for HA growth. In particular, Makyoh appears to be a useful complementary tool for optical microscopy for inter-sample comparison and for selecting a proper surface area for other studies.

Acknowledgements

The work in Budapest was supported, in part, by the Hungarian Scientific Research Fund (OTKA) under Grants T037711 and M041735 as well as by the Agency for Research Fund Management and Research Exploitation (KPI) under contract GVOP-3.2.1.-2004-04-0337/3.0. Sample preparation and modification was carried out in Bulgaria and supported by the Bulgarian National Scientific Research Fund through Grant L1213/2002 and by a Marie Curie grant No HPMT-CT-2000-00182 of the European Community.

References

- [1] L. L. Hench, J. Polak, *Science* **295**, 1014 (2002).
[2] D. M. Brunette, B. Chehroudi, *J. Biomech. Eng.* **121**, 49 (1999).
[3] F. Riesz, *Proc. SPIE* **5458**, 86 (2004).
[4] F. Riesz, *Mater. Sci. Eng. B* **80**, 220 (2001).
[5] I. E. Lukács, F. Riesz, *Eur. Phys. J. Appl. Phys.* **27**, 385 (2004).
[6] R. S. Sirohi, Fook Siong Chau, *Optical methods of measurement*, Marcel Dekker, New York (1999).
[7] L. Pramatarova, E. Pecheva, *Modified Inorganic Surfaces as a Model for Hydroxyapatite Growth*, Materials Science Foundations Series, **Vol. 26**, Trans Tech Publications, Zurich (2006).
[8] L. Pramatarova, E. Pecheva, R. Presker, U. Schwarz, R. Kiepe, *Solid State Phenom.* **106**, 75 (2005).

*Corresponding author: riesz@mfa.kfki.hu